Design and Optimisation of the Smart Pressure Sensor

Teboho Lekeno (1130992) **Partner: Kwena Mtshali (877040)**

School of Electrical & Information Engineering, University of the Witwatersrand, Private Bag 3, 2050, Johannesburg, South Africa

Abstract: This paper presents the design and analysis of a smart pressure sensor. The system incorporates vital subsystem such as signal sensing, conditioning, processing, data storage and additional implementation of self-calibration. The overall circuit has the static error of 2.31% and the dynamic error of 7.37%. The bandwidth of the system is obtained to be 4.5716kHz, which satisfy the minimum requirement of 1kHz. The system managed to satisfy the intrinsically safe standard and other SANS standards, the whole system is therefore deemed successful.

Key words: Anti-aliasing, Butterworth filter, South African National Standards (SANS),

1. INTRODUCTION

Power transformers are one of the most dangerous electrical equipment because of the large quantity of oil they contain which is in direct contact with the high voltage electrical components. When the oil losses its dielectric properties to limit electric field strength, low impedance faults occur resulting in electrical discharge. The discharge vaporizes the oil resulting in pressure accumulation inside the tank since the oil inertia prevents its expansion. The tank explosion occurs when the force exerted by the pressure exceed the force the tank walls can withstand, thus enabling the partial discharge to ignite the pressurized gases, resulting in the explosion. This paper therefore aims to design a smart pressure sensor to measure the pressure inside the HV transformer tank, which will allow the maintenance team to know when to service the transformer before an explosion can occur.

2. BACKGROUND

2.1 Constraints and Assumptions

To limit the scope of the design the following constraint and assumptions are imposed.

- Only primary sensors should be used.
- The system is build to measure pressure within transformer tank exploding at the not greater than 150psi.
- Mineral oil is the gas used inside the transformers.

2.2 Success Criteria

The integrated smart sensor system should have a minimum bandwidth of 1kHz. The smart sensor should have all elements contained in Bentley's measurement system generalized model. The system should conform with SANS in relation to general requirements (SANS 60079-0), level of protection (SANS 60079-11) and intrinsically safe electrical system (60079-25).

2.3 Literature Review

The dynamic characteristics of the pressure sensor are influenced by the connecting tube [1, 2]. The knowledge of dynamic characteristic of the measurement system allows the forecasting of the measurement out when input measured changes with time and allow the ability to determine the dynamic measurement error so that calibration can be imposed [3].

3. SPECIFICATIONS OF THE PRIMARY SENSOR

3.1 Static Specifications

Table 1 below shows the static characteristics of the primary sensor employed. The response time of the sensor is given to be 100μs, which gives it the bandwidth of 10kHz.

Table 1: Static specifications of SCX150AN pressure sensor

Parameter	**Value**	**SI unit**
Operating Pressure	0 to 150	psi
Sensitivity	1.0	mV/psi
Response Time	100μ	s
Supply voltage	20	Vdc
Full-Scale Span	90±1	mV
Compensated Operating Temperature	0 to 70	°C
Operating Temperature	-40 to 85	°C

3.2 Dynamic Specifications

Before the smart pressure sensor can be designed, it is necessary to determine the dynamic characteristics to properly adjust the measurement process. Figure 6, Appendix A shows the schematic of the pressure sensor with its connecting tube. The fluid in tube acts as the mass oscillator and the oscillator spring is imitated by the compressible fluid in the cavity which therefore forms a dynamic system which its derivation is shown on Appendix A. The corresponding transfer function for the dynamic characteristics is shown by equation 1 below.

$$H_1(s) = \frac{4.024 \times 10^9}{s^2 + 6.258 \cdot s + 4.023 \times 10^9} \tag{1}$$

The result is obtained using the connecting tube dimensions of primary pressure sensor aforementioned. The density, viscocity, and the speed of sound of the Mineral oil also applied to obtain the result [4]. The response time and bode-plot which characterizes the inlet pressure relationship with the actual pressure measured by the primary sensor are shown by Figure 1 and 2 below.

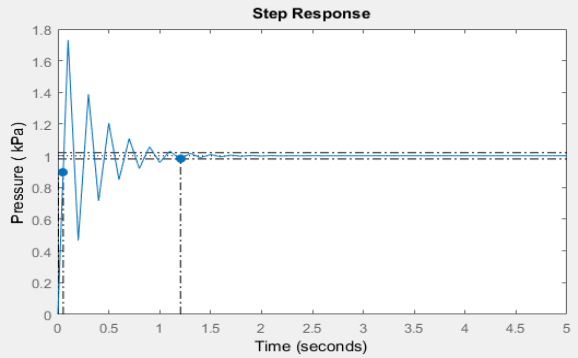

Figure 1: Step response for inlet pressure in tube and measured pressure

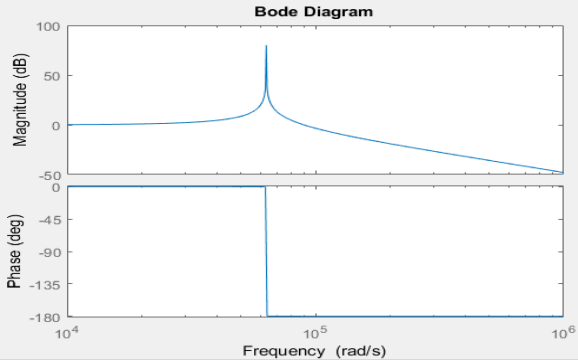

Figure 2: Bode-plot for inlet pressure and measured pressure transfer function.

The frequency of fluid is calculated to be 10kHz, using MATLAB. It is observed from Figure 1 that actual pressure measured will contain high noise with an overshoot of 73.1%, which settles after 1.2s. Using Figure 2 it is observed that the error of the measured fluid is within the range of 40000 rad/s and 62300 rad/s, of which is within the bandwidth of the primary sensor. The bode-plot and step response further show that maximum error has a gain of 80dB. The mitigation technique is necessary to eliminate the measured errors from the final.

4. DESIGN OF THE PRESSURE SENSOR

4.1 Low Pass Butterworth Filter

The SCX pressure sensor is found to have the peak to peak output noise of 1μV [5]. The noise is small compared to the voltage output of the sensor which is in millivolts. The nois can be ignored since its availability add no significant distortion to the measured results. The filter is therefore required to remove the noise from the output of the primary sensor caused by the tube as aforementioned. Since the error is found to reside within the bandwidth closer to the sensor's bandwidth, it is thus important to apply the low pass filter to attenuate the magnitudes at high frequencies causing the distortion and allow the lower frequencies to pass. The Butterworth filter allows any order, which introduces many poles that assist with faster attenuation of noise compared and does not consume input signal energy to operate compared to the low passive filter [6–8]. Table 1 below shows the design requirements of the filter.

Table 2: Design specifications for low pass Butterworth filter

Parameter	**Value**	**SI unit**
Pass band gain (G_p)	2.94	dB
Stop band gain (G_s)	-16.32	dB
Pass band frequency (ω_p)	3.39×10^4	rad/s
Stop band frequency (ω_s)	6.35×10^4	rad/s

The pass gain of 2.94 dB is used instead of the of 0 dB gain. Selecting the passing gain less than the selected one reduces the bandwidth of the input. Attenuating the signal bandwidth affects the signal measured since 70% of its data is stored within the bandwidth [9]. The calculated transfer function of the filter is shown by equation 2 below, which is 3^{rd} order Butterworth filter. The calculation performed to obtain the filter are shown Appendix A.

$$H_2(s) = \frac{4.024 \times 10^{13}}{s^3 + 68530.7s^2 + 2.348 \times 10^9 s + 4.024 \times 10^{13}} \quad (2)$$

With the transfer function of the filter now obtained, it is now necessary to determine the filtered output which will be processed, to achieve that, the dynamic characteristic transfer function is cascaded with the filter transfer function. The obtained results are showcased by Figure 3 and 4 below.

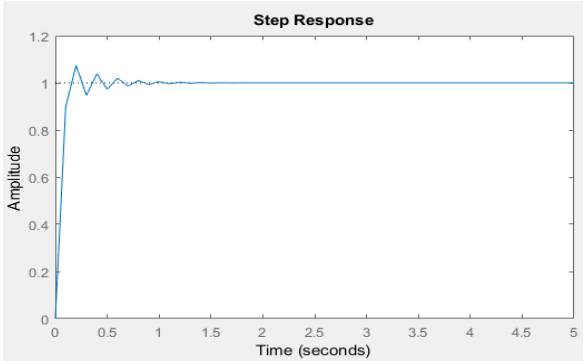

Figure 3: Step response for inlet pressure in tube and filtered measured pressure

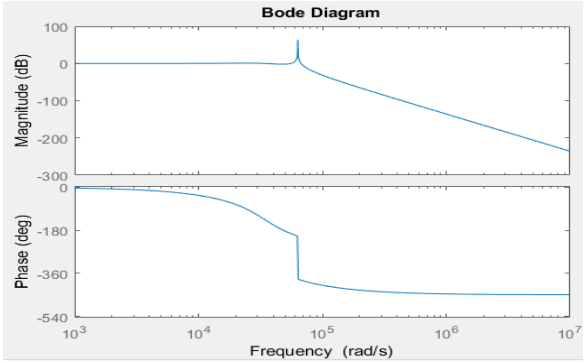

Figure 4: Bode-plot for inlet pressure and filtered measured pressure transfer function.

The noise of the pressure measured is reduced as shown in Figure 3 compared to Figure 1. The settling time of the noise is reduced by 60% to 0.5 seconds and the overshoot is improved from 73.1% to 7.37%. The bode-plot also shows a constant gain and the attenuation per decade of higher frequencies being increased without distorting the energy within the bandwidth of the measured signal as designed.

4.2 Primary Sensor Output Amplification

The amplification of the primary sensor output signal is affected by the reference voltage of the A/D conversion selected. To improve the readability of the analogue input, the A/D reference voltage of 2.048V is selected and the resolution of 1023 using 10 bits. Since the primary sensor can measure up to 150 psi with sensitivity aforementioned, it is necessary to amplify the maximum output voltage the sensor to be equivalent to the reference voltage to retain the required readability. Equation 3 is used to determine the required gain of the amplifier, of which it will be non-inverting.

$$Gain = \frac{V_o}{V_i} = 1 + \frac{R_f}{R} \tag{3}$$

Where V_i is the filtered output voltage from the sensor, V_o is the output voltage from the amplifier, R_f and R are desired resistors to give the required gain. Using maximum primary sensor output voltage of 150mV and requiring it to be amplified to 2.048V, the corresponding amplification gain is obtained to be 13.6533. This implies selecting the value of R to be 1kΩ gives the R_f value of 12.6533kΩ. Equation 4 below is used to determine the digital sensitivity of the system, which is calculated to be 6.82.

$$Digital_{sensitivity} = \frac{Resolution}{V_{reference}} \times Gain \times sensitivity \tag{4}$$

4.3 Signal Processing

The averaged and amplified signal from the primary sensor is processed in this phase using the Microchip. This chip will allow conversion of the signal from analogue to digital, which further allows necessary calculations using digital values to obtain the pressure of the measurand and later display it.

4.3.1 ***Anti-aliasing*** When sampling the analogue data during A/D conversion it is required to prevent aliasing of the sampled data for reliability and accuracy of measurement [10]. To prevent aliasing and loss of data, the sampling frequency of the sampler should at least be twice the frequency of the sampled signal [11]. The minimum sampling frequency of the PIC micro-controller should then be 20kHz since the frequency of the fluid measured will be at 10kHz. Any Atmega micro-controller cannot be used in this stage since their maximum achievable sampling rate is 9615 Hz with a 16 kHz EXTAL frequency [12]. To prevent Aliasing, dsPICFJ256GP710A Microchip is selected since it has the maximum sampling rate of 1.1 MHz for A/D with 40 million instructions per seconds [13, 14].

4.3.2 ***Calibration*** There are a variety of self-calibration techniques for smart sensors such as background calibration, differential sensing, and cross-sensitivity compensation [15]. The cross-sensitivity technique will be applied, for which the measuring primary sensor is the function of pressure and temperature. Temperature influence the sensitivity and zero-bias point of the sensor. It is also observed from sensor static specifications that it is calibrated for ranges of temperature between 0°C to 70°C, for temperatures out of that range the sensor will give false data, therefore the temperature sensor is required to give knowledge of the temperature to the system.

The response of the LM35 temperature sensor is approximately 2 seconds [16], therefore, to improve the response time of the total system, the temperature will be measured and converted to digital value every 2 seconds.

The micro-controller look-up tables will be used to store different temperatures and there will be two other look-up tables for storing the sensitivity and offset values corresponding the temperatures. If the temperature changes; its corresponding sensitivity and the offset will be selected from their respective vectors and applied to replace the previous sensitivity and offset values.

Additional calibration added to the design, is the use of average amplifier. Instead of using a single pressure sensor. Four sensors will be used and average within the non-inverting amplifier.

Figure 5 below showcases the flow diagram of the signal processing with auto-calibration.

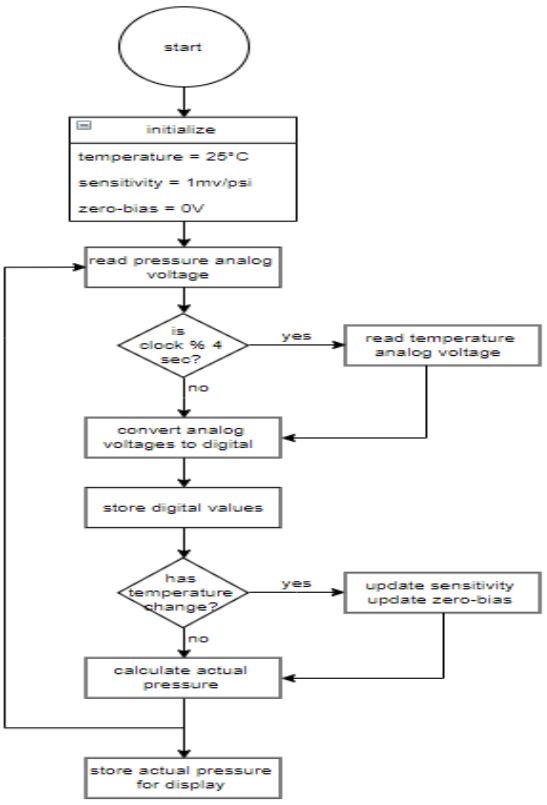

Figure 5: Signal processing with cross-sensitivity auto-calibration

4.3.3 ***Handling Overflow*** If the output voltage from the amplifier is greater than that the reference voltage of the A/D conversion, the overflow within the ADCH register in the microcontroller will overflow which results in the incorrect processing of data. The amplifier was designed for normal sensor sensitivity of 1mv/psi. Assuming temperature increases from the normal calibrated 25^oC and the sensitivity of the sensor drift 1.2mV/psi, if the pressure measured is currently 150psi, its corresponding amplified voltage detected by the microcontroller will be 2.4576V which is greater than the reference voltage selected. using equation 4, it is clear that the digital voltage value will be 1227.6, which is greater than the specified resolution value. This means the overflow will occur and the value that will be read is 1227.6 - 1023 which equal to 204.6 which is less than 150psi when converted as shown by equation 5 below.

$$P = \frac{digital \quad pressure}{digital \quad sensitivity} = \frac{204.6}{6.82} = 30psi \qquad (5)$$

To prevent loss of the processed data due to overflow, for every A/D conversion taking place, the overflow flag within the microcontroller will be monitored. If the flag is set (equal to 1), the 16-bit register will be used and 1023 will be added to register to compensate for the overflow. Finally, the remaining value in ADC registers will also be added to 16-bit register to complete the actual digital value processed.

4.4 Data Presentation

The LCD Module 2004A is employed for data presentation. The model operates with 5Vdc. It has the rise time of $25ns$, data output delay of $360ns$ and display format of 20 characters $\times$ 4 lines [17]. It will use the output received from the Microchip to display the measured pressure in *psi*.

Figure 7, Appendix B showcases the complete smart pressure sensor circuit.

5. SPECIFICATIONS OF THE SMART PRESSURE SENSOR

5.1 Static Characteristics

Table 3: Static specifications of the smart pressure sensor

Parameter	**Value**	**SI unit**
Operating Pressure	0 to 150	psi
Sensitivity	1.0	mV/psi
Response Tine	218.7μ	s
Full-Scale Span	90 ± 1	mV
Compensated Operating Temperature	-40 to 85	°C
Operating Temperature	-40 to 85	°C

5.2 Dynamic Characteristics

The system overall dynamic response constitute of the pressure sensor dynamics and the signal conditioning. The transfer function of the entire system is then the cascade of the two, including the gain of the amplifier as shown by (6) below.

$$H_3(s) = \frac{a}{s^5 + bs^4 + cs^3 + ds^2 + es + f} \qquad (6)$$

- a = 22.1047×10^{23} $b = 6.854 \times 10^4$ $c = 6.372 \times 10^9$
- d = 3.16×10^{14} $e = 9.447 \times 10^{18}$ $f = 1.619 \times 10^{23}$

To determine the bandwidth of the entire system, it is important to consider the time it takes the microchip to process the data and also include the response of the LCD display as well. Equation 7 below allows the calculation of the entire system bandwidth to be determined [18].

$$f_{3dB} = \left[\frac{1}{f_{tube}^2} + \frac{1}{f_{sensor}^2} + \frac{1}{f_{filter}^2}\right]^{-\frac{1}{2}} \qquad (7)$$

With the knowledge of wide-bandwidth of cascaded systems aforementioned, the total bandwidth of the system is calculated to be 6.307kHz.

6. STANDARD

To reduce the noise of the pressure measured the pressure sensor will be installed directly inside the tank, this reduces the length of the connecting tube thus improving dynamic response. To ensure that the installation of the primary pressure sensor inside the tank does not contribute to an explosion, the following measures are considered.

6.1 Flame Proof Enclosure and Oil-Immersion

The sensor is powered using 20Vdc, short circuit of this voltage is high enough to ignite gases formed inside the transformer. SANS 60079-14, IEC 60079-10-1, and IEC 60079-10-2 argues that an enclosure is necessary for such equipment's and methods such as immersing the equipment inside the oil can be applied [19]. The sensor will then be located at the bottom of the tank.

6.2 Protection against Lightning and other Electrical Surges

If the conductor supplying power from the main circuit outside the transformer tank to the sensor inside the tank is strike by lightning, the impulse induced by the lightning will further cause partial discharge and damage the sensor. SANS 60079-25 encourage the use of surge protection device capable of diverting minimum peak current of 10kA. The CBI surge protection breaker should there be used since it satisfies the peak current specifications [20]. The surge protection device should also be installed according to SANS 60079-25, which state that one surge arrester should be outside but close to the boundary of the explosive environment, this will trap all the current directly to ground and prevent sensor damage and partial discharge.

7. CRITICAL ANALYSIS

7.1 System Dynamic Characteristic

The bandwidth of 4.5716kHz was obtained for the overall system. With the fluid measured and dimensions of the primary sensor tube, the response of the actual pressure measured by it was obtained to overshoot by 73.1%, which settle after 1.2 s. With the application of the Butterworth filter, the total system overshoot was reduced to 7.37% and the settling time reduces to 0.516 s. This means the system will now quickly respond to the change in pressure but the noise will be noticed for 0.516 s before it settles.

7.2 Error Analysis

Table 4: System static error contributions.

System Component	Error
Primary sensing element	1.11%
Average amplifier	1.20%
Overall system error	2.31%

7.2.1 ***Static Errors*** The static errors to the system are introduced due to parasitic effects on the average amplifier and errors in the full-scale span of the sensor. Table 3 shows these elements their corresponding errors obtained. An overall system error of 2.31% is obtained.

7.2.2 ***Dynamic Errors*** The system has the overshoot of 7.37% and the settling time of 0.516s. The contributor of the dynamic error was witnessed to be the connecting tube of the pressure sensor, of which the sensing element already measure pressure with noise.

8. SOCIAL ETHICS

The whole system will not contribute to partial discharge which will cause an explosion due to abiding by the requirements of SANS 60079-25. The primary sensor is mounted at the base of the tank to ensure it is immersed in oil and does not contribute to ignition of gases above the oil surface, which satisfy the requirements of SANS 60079-14, IEC 60079-10-1, and IEC 60079-10-2. This will ensure that the measurement system carry its own duty without damaging the environment which makes the system to be environmental friendly.

9. FUTURE RECOMMENDATIONS

Due to the length of the pressure sensor being directly proportional to the percentage overshoot of the actual pressure measured. The efficiency of the overall measurement system can be improved by obtaining a sensor with small tube length but achieving the similar static specifications.

10. ACKNOWLEDGEMENT

This project was successfully completed by teamwork. To complete the project within the project schedule, the project subsystem where divided between group members. Kwena Mtshali with designing of the Butterworth filter to remove the noise from the output of the season and the design of the amplification system. I then handle the signal processing which incorporates of A/D conversion, prevention of aliasing and the calibration of the system as well. The project plan was well planned at the group members collaborated on GitHub to allow flexible work and to go back in time in case any unwanted changes were saved on the work-space.

11. CONCLUSION

The smart pressure sensor to measure the pressure inside the HV transformer has been presented. The final system has the bandwidth of 4.5716kHz which satisfy the requirements of the projects. The systematic errors for both the static and dynamic are found to be 2.31% and 7.37% respectively. The cross-sensitivity calibration technique was applied to allow the system to determine temperature, then uses it to choose its corresponding sensitivity and bias. The system is found to comply with all the SANS standards imposed and it is therefore deemed intrinsically safe.

REFERENCES

[1] J. Hjelmgren. *Dynamic measurement of pressure.-A literature survey*. 2002.

[2] S. A. Whitmore and C. T. Leondes. "Pneumatic distortion compensation for aircraft surface pressure sensing devices." *Journal of Aircraft*, vol. 28, no. 12, pp. 828–836, 1991.

[3] I. Bajsić, J. Kutin, and T. Žagar. "Response time of a pressure measurement system with a connecting tube." *Instrumentation Science and Technology*, vol. 35, no. 4, pp. 399–409, 2007.

[4] H. Jin, T. Andritsch, I. A. Tsekmes, R. Kochetov, P. H. Morshuis, and J. J. Smit. "Properties of mineral oil based silica nanofluids." *IEEE Transactions on Dielectrics and Electrical Insulation*, vol. 21, no. 3, pp. 1100–1108, 2014.

[5] S. Technics. "SCX Series: Precision compensated pressure sensors.", aug 2005. URL `https://datasheet.octopart.com/SCX15DN-Honeywell-datasheet-5336229.pdf`.

[6] J. Karki. "Active low-pass filter design." *Texas Instruments application report*, 2000.

[7] W.-K. Chen. *Passive, active, and digital filters*. Crc Press, 2009.

[8] D. Simon. "Training fuzzy systems with the extended Kalman filter." *Fuzzy sets and systems*, vol. 132, no. 2, pp. 189–199, 2002.

[9] M. A. Halim and J. Y. Park. "Theoretical modeling and analysis of mechanical impact driven and frequency up-converted piezoelectric energy harvester for low-frequency and wide-bandwidth operation." *Sensors and actuators A: physical*, vol. 208, pp. 56–65, 2014.

[10] J. Korein and N. Badler. "Temporal anti-aliasing in computer generated animation." In *ACM SIGGRAPH Computer Graphics*, vol. 17, pp. 377–388. ACM, 1983.

[11] Q. Tu and Z. Xu. "Impact of sampling frequency on harmonic distortion for modular multilevel converter." *IEEE Transactions on Power Delivery*, vol. 26, no. 1, pp. 298–306, 2011.

[12] Atmega. "ATmega328P - 8-bit AVR Microcontrollers.", jan 2019. URL `https://www.microchip.com/wwwproducts/en/ATMEGA328P`.

[13] M. T. Inc. "dsPIC33F Family Data Sheet: High-Performance, 16-bit Digital Signal Controllers.", jan 2005. URL `http://ww1.microchip.com/downloads/en/devicedoc/70165a.pdf`.

[14] T. Fredriks. "Ultrasonic Listener: Microcontroller Based Frequency Shifter." 2010.

[15] M. Pertijs. "Calibration and Self-Calibration of Smart Sensors." *Smart Sensor Systems: Emerging Technologies and Applications*, pp. 17–41, 2014.

[16] T. Instruments. "LM35 Precision Centigrade Temperature Sensors.", jan 2015. URL `http://henrysbench.capnfatz.com/wp-content/uploads/2015/05/lm35-datasheet.pdf`.

[17] S. E. ELECTRONICS. "Specification For LCD Module 2004A.", sep 2007. URL `https://www.beta-estore.com/download/rk/RK-10290_410.pdf`.

[18] A. Hollister. "Wolfram Demonstrations Project.", Mar 2011. URL `http://demonstrations.wolfram.com/SystemBandwidthForCascadedAmplifiers/`.

[19] S. A. N. STANDARD. "Part 14: Electrical installations design, selection and erection." *Explosive atmospheres*, p. 11124, May 2014. URL `http://sabs.wits.ac.za/documents/SANS60079-14.pdf`.

[20] "CBI Surge Protection Breaker." URL `https://www.builders.co.za/Electrical/Plugs-&-Extension-Cords/Surge-Protection/CBI-Surge-Protection-Breaker/p/0000000000000381063?gclid=EAIaIQobChMIt-eu86WJ4gIVZzbTCh1YqwK_EAQYBiABEgJTgPD_BwE`.

Appendix A

Derivation of the Dynamic Characteristics of the Pressure Sensor

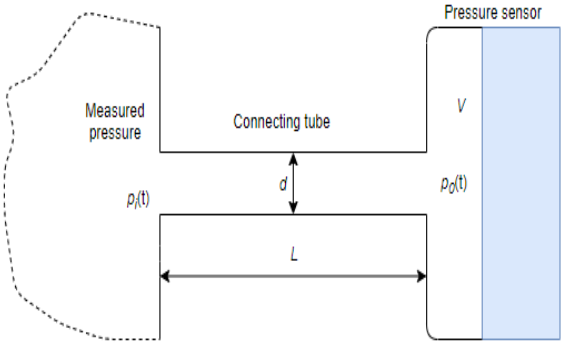

Figure 6: Pressure sensor with connecting tube schematic diagram

$$\frac{d^2\rho_o}{dt^2} + 2\zeta\omega_0\frac{d\rho_o}{dt} + \omega^2\rho_0 = \omega^2\rho_i \tag{8}$$

where $\omega_0 = 2\pi f_0$ is the natural angular frequency and ζ is the damping ratio.

The natural frequency and the damping ratio are expressed by equation 9 and 10 below,

$$f_0 = \frac{C}{2\pi}\sqrt{\frac{A}{L \times V_{ef}}}, \qquad V_{ef} = V + \frac{L \times A}{2} \tag{9}$$

$$\zeta = \frac{2\mu}{f_0 \times \rho \times A} \tag{10}$$

where μ is the dynamic viscosity and ρ is the fluid density at inlet parameters.

Third Order Butterworth Filter

$$A_{mag} = 10^{\frac{G_p}{20}} = 10^{\frac{2.94}{20}} = 1.4028 \tag{11}$$

$$\epsilon = \sqrt{A_{mag}^2 - 1} = 0.968 \tag{12}$$

$$H(jw) = \frac{H_o}{\sqrt{1 + \epsilon^2(\frac{\omega_s}{\omega_p})^{2n}}} \tag{13}$$

The minimum stop band gain G_s = -16.32dB which is equal to a gain of 6.54 at a stop band frequency 6.35×10^4 rads/s. Using equation 14, the value of order of filter is obtained as show below.

$$\frac{1}{6.54} = \frac{1}{\sqrt{1 + 0.968^2(\frac{6.35}{3.39})^{2n}}}, \quad n = 3 \tag{14}$$

The cut-off frequency of the filter is obtained using equation 15 below, with ω_p = 33.9k rads/s.

$$\omega_c^3 = \frac{\omega_p^n}{\epsilon}, \quad \omega_c = 3.4269 \times 10^4 rad/s \tag{15}$$

$$H(s) = \frac{1}{(\frac{s}{\omega_c}^3) + 2(\frac{s}{\omega_c})^2 + 2(\frac{s}{\omega_c}) + 1} = \frac{4.024 \times 10^{13}}{s^3 + 68530.7s^2 + 2.348 \times 10^9 s + 4.024 \times 10^{13}} \tag{16}$$

Appendix B

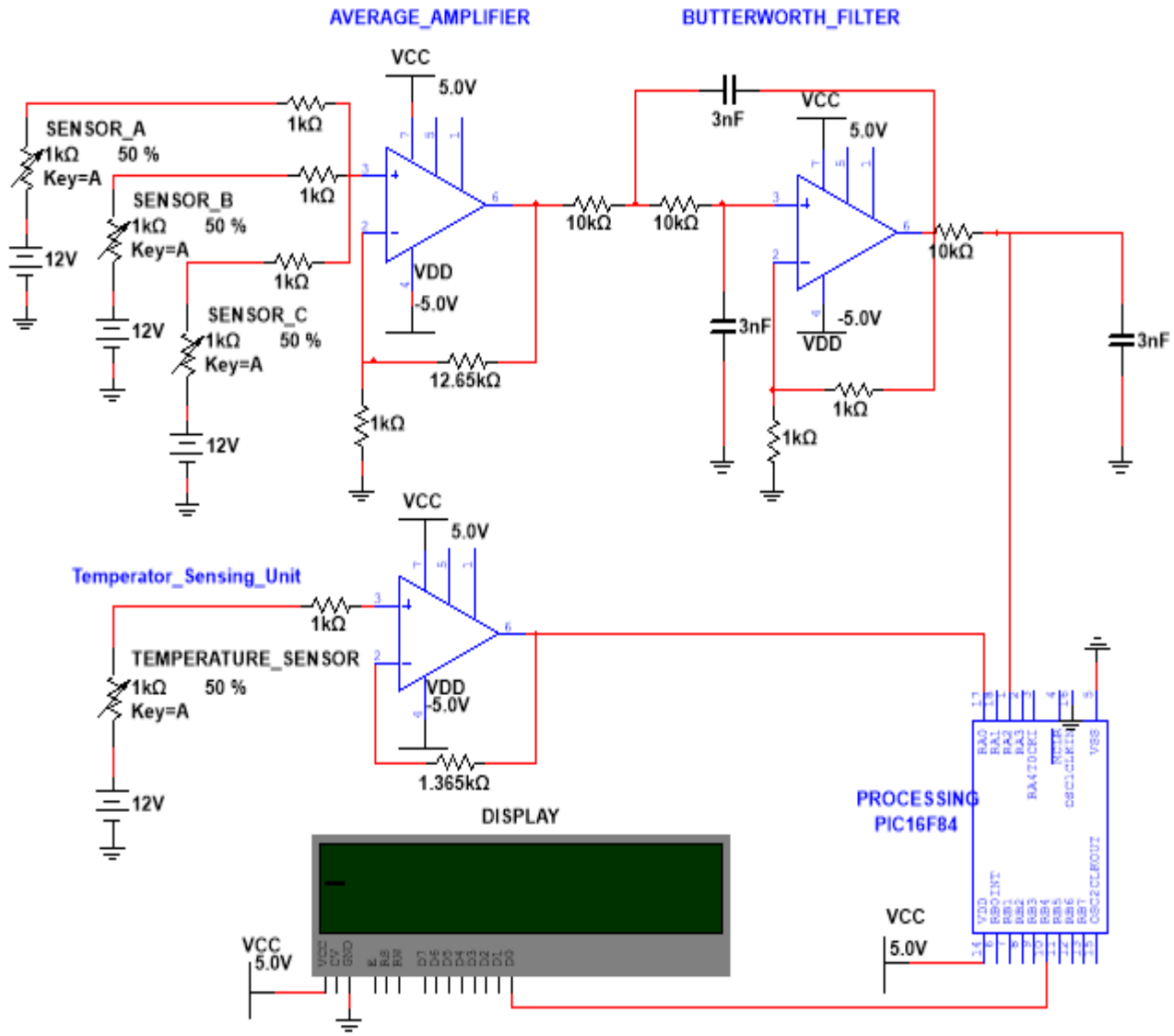

Figure 7: Smart pressure sensor circuit diagram